ARTICLE

OPEN

Check for updates

The relative role of the subsurface Southern Ocean in driving negative Antarctic Sea ice extent anomalies in 2016–2021

Liping Zhang [1,2 ✉], Thomas L. Delworth [1], Xiaosong Yang[1], Fanrong Zeng[1], Feiyu Lu[1,3], Yushi Morioka[1,3,4] & Mitchell Bushuk[1,2]

The low Antarctic sea ice extent following its dramatic decline in late 2016 has persisted over a multiyear period. However, it remains unclear to what extent this low sea ice extent can be attributed to changing ocean conditions. Here, we investigate the causes of this period of low Antarctic sea ice extent using a coupled climate model partially constrained by observations. We find that the subsurface Southern Ocean played a smaller role than the atmosphere in the extreme sea ice extent low in 2016, but was critical for the persistence of negative anomalies over 2016–2021. Prior to 2016, the subsurface Southern Ocean warmed in response to enhanced westerly winds. Decadal hindcasts show that subsurface warming has persisted and gradually destabilized the ocean from below, reducing sea ice extent over several years. The simultaneous variations in the atmosphere and ocean after 2016 have further amplified the decline in Antarctic sea ice extent.

[1] NOAA/Geophysical Fluid Dynamics Laboratory, Princeton, NJ, USA. [2] University Corporation for Atmospheric Research, Boulder, CO, USA. [3] Atmospheric and Oceanic Science, Princeton University, Princeton, NJ, USA. [4] Application Laboratory, VAiG, JAMSTEC, Yokohama, Japan. ✉email: Liping.Zhang@noaa.gov

Antarctic sea ice is characterized by large variations in areal extent, with substantial implications for the exchange of energy, momentum, and gas between the atmosphere and the ocean[1]. Antarctic sea ice varies on broad timescales from subseasonal to decadal and has a long-term trend as well[2–7]. Satellite observation (1979-now) shows Antarctic Sea ice extent (SIE) reached a record high in 2014 and then rapidly dropped to a record low in late 2016 (Fig. 1a). Prior to 2014, total Antarctic SIE had a small positive linear trend over the satellite era, with large regional variability[8–11]. This is in stark contrast to the declining Arctic Sea ice[12,13]. Moreover, the trend for SIE expansion accelerated after 2000 by almost a factor of five relative to the trend for 1979 to 1999[14]. Several hypotheses have been proposed to explain this observed positive trend, including surface wind anomalies induced by the Southern Annual mode (SAM) or tropical SST anomalies[15–22], a freshening of the Southern Ocean (SO)[23–28], internal variability[29–31], the role of mesoscale eddies[32], and successful simulations of sea ice drift velocity[33] and SO SST[34]. The accelerating rate of sea ice expansion during the post-2000 period is suggested to be related to the negative phase of the interdecadal Pacific oscillation (IPO) that can induce atmosphere teleconnection patterns and thus alter the surface wind anomalies over the SO[14]. A recent study showed that this increasing trend over satellite period is opposite to the longer-term variability in

the recent century-long reconstruction[35]. A linear trend might not be the best way to describe the long-term variability in Antarctic SIE[36].

After 2014, Antarctic SIE started to decrease and dramatically dropped to a record low in late 2016[37–43], after which the unexpected low sea ice state persisted for several years (Fig. 1a). In February 2022, the SIE reached a new record low[44]. Observations and model experiments by prescribing observed tropical SST anomalies suggested that the 2016 extreme sea ice low was caused by (1) southward warm air advection associated with the zonal wave number 3 teleconnection pattern in the early austral spring induced by tropical SST anomalies, and (2) the strong negative SAM event in the late austral spring[38–42]. By analyzing sparse ocean observations, previous studies also pointed out that the decadal-long SO warming associated with the SAM and IPO may contribute to the sudden Antarctic SIE decline and sustain a persistent sea ice decrease[43]. However, it is not clear to what extent this sudden SIE decline can be attributable to the local ocean, particularly the subsurface SO, or the relative role of the subsurface SO compared to the atmosphere contribution. There is also no answer on whether the subsurface heat is large enough to overwhelm the surface ocean variability. We are also not clear if the subsurface SO could lead to potential predictability of the persistent Antarctic SIE declines given the long memory of subsurface ocean.
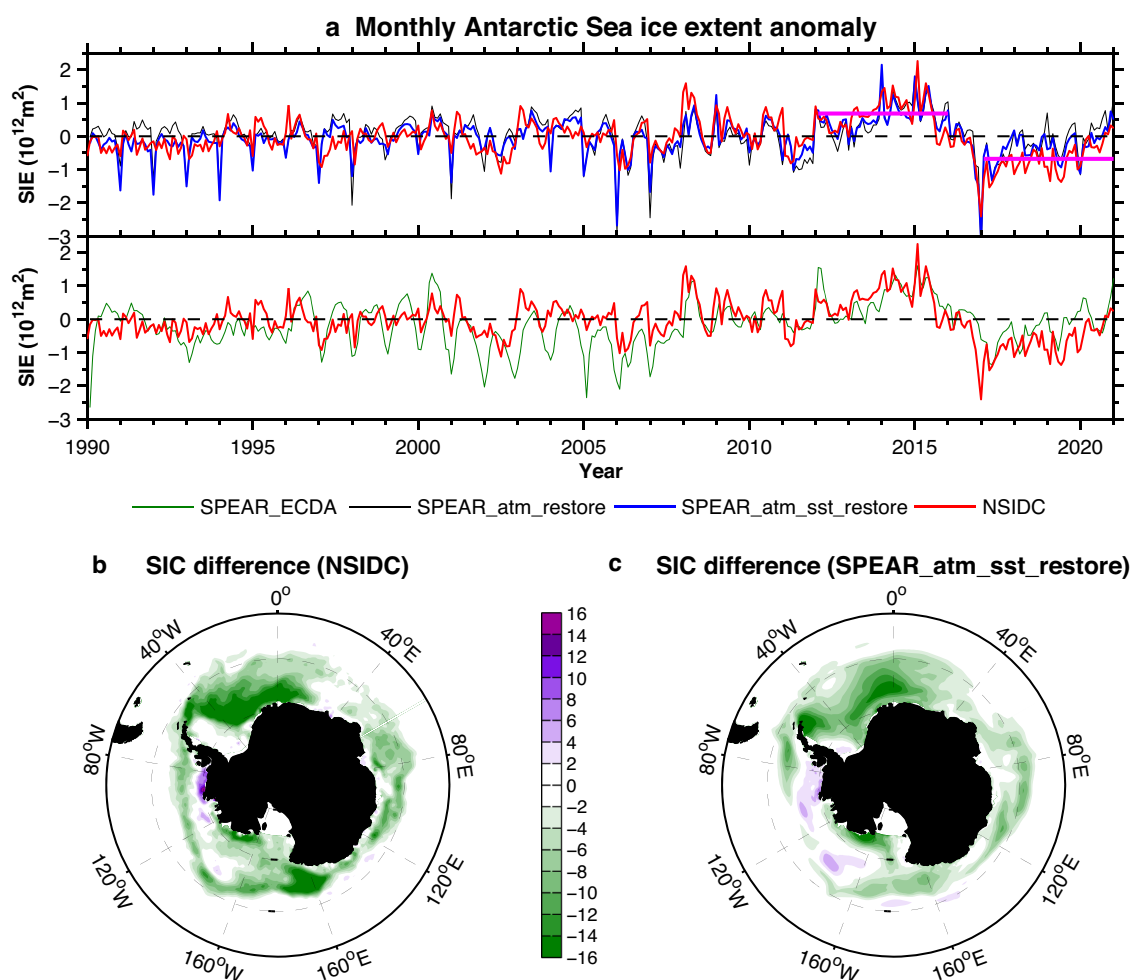

Fig. 1 Variability in Antarctic Sea ice extent (SIE) derived from observations and SPEAR model simulations. a Monthly mean SIE anomaly since 1990 with respect to the 1990–2020 climatology in SPEAR_ECDA (green line), SPEAR_atm_restore (black line), SPEAR_atm_sst_restore (blue line), and National Snow and Ice Data Center (NSIDC) observation (red line). Magenta lines are the time averages of SIE anomalies over the time period 2012–2015 and 2017–2020 in NSIDC. **b** Sea ice concentration (SIC) difference between time period 2017–2020 and 2012–2015 in NSIDC. **c** Same as (**b**) but in SPEAR_atm_sst_restore. Units are $10^{12}m^2$ for SIE and % for SIC.

In this study we use a suite of Geophysical Fluid Dynamic Laboratory (GFDL) SPEAR model simulations[45] partially constrained by observations, along with sensitivity experiments (see "Methods" and Table 1 for model details), to evaluate the relative role of the subsurface SO in the recent Antarctic SIE declines. We also use initialized decadal hindcasts/forecasts[46] with the SPEAR model to investigate the role of the ocean in determining sea ice cover. We find that the subsurface Southern Ocean (SO) plays a smaller role in the 2016 SIE extreme event than the atmosphere. However, the subsurface SO is critical to the persistence of the negative SIE anomalies after 2016.

Results

Simulated Antarctic SIE variability in the GFDL SPEAR models. We show in Fig. 1a the time series of monthly Antarctic SIE anomalies in observations and various model simulations. Note that the SPEAR models we used here well simulate the sea ice climatology compared to observation (Supplementary Figs. S1, S2). The SIE climatology generally has a low bias in austral summer and a high bias in austral winter, or moderate high biases throughout all seasons, which are very common in coupled models (Supplementary Fig. S1). The simulated Antarctic sea ice concentration (SIC) is broadly like that in observation in all seasons, with high spatial correlations with observation (Supplementary Fig. S2). The SIE anomaly in each model is the deviation from each model's monthly SIE climatology. The sea ice evolution in SPEAR_atm_sst_restore (see "Methods" and Table 1 for details) that is constrained by atmospheric and SST observations is highly correlated with NSIDC, with a correlation reaching 0.75 ($p < 0.05$) during the period 1990–2020. The SPEAR_atm_sst_restore captures the observed record low SIE in late 2016, and also successfully reproduces the sea ice shift in the most recent decade, with positive SIE anomalies during 2012–2015 and negative SIE anomalies during 2017–2020, albeit with a higher SIE in that later periods compared to observations. The SPEAR_atm_restore, constrained by atmospheric observations but without ERSST restoring, is still able to capture the observed SIE long-term trend, extreme event, and the recent shift. The correlation reaches 0.69 ($p < 0.05$) and 0.9 ($p < 0.05$) when comparing with the observations and SPEAR_atm_sst_restore, respectively. These high correlations suggest that the SST restoring north of 60°S does not affect the Antarctic SIE variability very much for the timescales assessed here. On the other hand, when we constrain our model with the ocean temperature and salinity observations but with a free atmosphere (SPEAR_ECDA), we find the SIE correlation with observation in this ocean data assimilation (cor = 0.6, $p < 0.05$) is lower than the previous two atmospheric constrained runs. This may partly arise from the insufficient ocean observations over the SO particularly in ice-covered regions that are not enough to fully constrain our coupled model. Surprisingly, the SPEAR_ECDA substantially underestimates the observed record low Antarctic SIE in late 2016. Apart from the insufficient ocean data constraints, this may also indicate that the atmosphere, such as internal atmospheric variability, may play a critical role in generating the observed record-breaking SIE extreme event. However, the SPEAR_ECDA broadly captures the SIE shift over the most recent decade, with relatively lower SIE states after 2016 compared to previous years, like that in SPEAR_atm_sst_restore and SPEAR_atm_restore.

To investigate why SPEAR_ECDA fails to reproduce the record low SIE in late 2016, we plot the SIC and sea level pressure (SLP) anomalies averaged in November and December (ND) 2016 (Supplementary Fig. S3a–d) in the SPEAR_atm_sst_restore, SPEAR_ECDA, and observations. In SPEAR_atm_sst_restore, there is a strong negative SAM event in 2016ND characterized by positive sea level pressure anomalies around Antarctica and this is

Table 1 Description of models used in the current paper.

Name	General information	Resolution	Simulation length	Reference
SPEAR_LO	Coupled model developed at GFDL. Ocn & Ice use MOM6-SIS2. Atm & Land are from AM4-LM4.	Ocn & Ice: ~1°, 75 vertical layers Atm & Land: 100 km, 33 levels	1–3000 year control run with fixed forcing	Delworth et al.[45] Adcroft et al.[56] Zhao et al.[57,58]
SPEAR_atm_sst_restore	Based on SPEAR_LO. 3-d atmospheric restoring towards JRA-55 and the SST restoring toward the ERSSTv5. Forced by historical radiative forcing.	Same as SPEAR_LO	Year 1958–2021 30 ensemble members	Yang et al.[46]
SPEAR_atm_restore	Based on SPEAR_LO. 3-d atmospheric restoring towards JRA-55 and with historical radiative forcing.	Same as SPEAR_LO	Year 1958–2021 5 ensemble members	Yang et al.[46]
SPEAR_ECDA	Based on SPEAR_LO. Ocean data assimilation in MOM6, with the ocean tendency adjustment bias correction scheme and a free atmosphere.	Same as SPEAR_LO	Year 1990–2021 30 ensemble members	Lu et al.[61]
SPEAR Decadal hindcasts/forecasts	Based on SPEAR_LO and initialized from SPEAR_atm_sst_restore. Forced by historical radiative forcing.	Same as SPEAR_LO	Initialized on 1 January every year from 1961 to 2021. 10-year run and 20 ensemble members.	Yang et al.[46]
SPEAR_atm_restore_2015_newIC	Identical to the SPEAR_atm_restore except that the ocean conditions on 1 January 2015 is replaced by that in another year.	Same as SPEAR_LO	Year 2015–2021 5 ensemble members	

in agreement with observations[38–41]. The negative SAM corresponds to a weakening of westerly winds over the SO, which reduces the turbulent heat loss and favors a southward Ekman transport and ocean heat transport, eventually leading to warming anomalies and SIE decline over the SO[40,41]. The scatter plot of SAM versus the Antarctic SIE in SPEAR_atm_sst_restore further exhibits that the more negative SAM over the SO, the lower the Antarctic SIE (Supplementary Fig. S3c). In stark contrast, we do not see a strong negative SAM event during this season in SPEAR_ECDA (no positive sea level pressure anomalies around Antarctica), for which the atmosphere is not constrained by observations. The absence of weakened westerly winds over the SO precludes the development in SPEAR_ECDA of the observed SIE extreme event, suggesting that wind-driven sea ice dynamics played a critical role in the 2016 event. Similarly, the SPEAR_ECDA underestimates the wave number 3 pattern during September and October (SO) 2016 characterized by three high and three low-pressure centers around the Southern Hemisphere extratropics because of tropical SST anomalies as mentioned by previous studies[41,42] compared to the SPEAR_atm_sst_restore and observations due to its unconstrained atmosphere (Supplementary Fig. S4a–d). In SPEAR_atm_sst_restore, the southward warm air advection and dynamical ice convergence associated with the wave number 3 pattern favors a warming of SO and thus a decrease of Antarctic SIE[38–43]. The year with stronger southward wind anomalies corresponds to a lower SIE and vice versa. By comparing the "perfect" atmosphere reanalysis (SPEAR_atm_sst_restore; SPEAR_atm_restore) with the "perfect" ocean reanalysis (SPEAR_ECDA), we conclude that the SAM and zonal wave number 3 pattern over the SO play dominant roles in the record low Antarctic SIE in late 2016.

To explore the persistent SIE declines after 2016, we look at the spatial pattern of SIC differences between 2017–2020 and 2012–2015 (Fig. 1b, c). The sea ice decline occurs in almost all ocean basins, with a maximum over the Weddell Sea. There is an exception over the Amundsen-Bellingshausen Seas which exhibits a small SIC increase in both observations and SPEAR_atm_sst_restore, with bigger increases farther north in the model. Similar characteristics of sea ice decrease are seen in other simulations (Supplementary Fig. S5). The SIE time series in different ocean basins further confirm the total SIE declines after 2016 and the biggest SIE shift over the Weddell Sea (Supplementary Fig. S6). Again, we can see the Amundsen-Bellingshausen Seas show an opposite sea ice response compared to other basins, with increasing SIE anomalies post-2017. Next, we will explore the role of the ocean in this persistently low Antarctic SIE in recent years. Given the dominant variability over the Weddell Sea, we also show the characteristics of Weddell Sea to make a comparison with the whole SO in the next section.

Role of ocean in the persistent Antarctic SIE declines. To highlight the most recent sea ice shift, we display in Fig. 2a, b the total Antarctic SIE and Weddell SIE anomaly time series since 2011, computed with respect to the 2011–2020 climatology. Interestingly, model simulations overall reproduce the persistent sea ice lows after 2016 and match the observation much better over the 2011–2020 period than the full period shown in Fig. 1a. This may benefit from the increased and improved observations in recent years, especially the ocean part (Supplementary Fig. S7), which can better constrain our model. We then show in Fig. 2c, e the SO area averaged temperature and salinity profiles in SPEAR_atm_sst_restore. Similar characteristics are also seen in other simulations (Supplementary Fig. S8). The persistent SIE negative anomalies after 2016 correspond to an overall warm and salty upper ocean. The SIE declines are preceded by a heat buildup in the subsurface ocean (depths of roughly 100–500 m) and a salinification in the surface ocean. Both the subsurface temperature and salinity anomalies tend to destabilize the upper ocean and trigger vertical instabilities. Note that the heat buildup we have seen here takes place in the upper 500 m, which is different from the convection occurrence in the deep ocean shown previously[47,48]. The Weddell Sea shows similar subsurface ocean features but with a larger magnitude (Fig. 2d, f), consistent with the maximum sea ice decline there (Fig. 1b, c). We also compare these SPEAR simulations with the EN4 reanalysis[49] (Supplementary Fig. S9). The subsurface warming and surface salinification signals before ND2016 are also seen in the EN4 reanalysis, although signals are nosier and intermittent presumably due to the presence of small-scale processes in the real ocean. The vertical mixing seems stronger in the EN4 than our models given the stronger penetration of surface temperature and salinity anomalies to the subsurface ocean. It is worth noting that there are still many uncertainties in the EN4 reanalysis, since the SO subsurface observations are very sparse, particularly over the Weddell Sea.

Heat budget analysis reveals that the SO subsurface (100–500 m) heat reservoir in Fig. 2c is largely due to horizontal and vertical temperature advection terms (Supplementary Fig. S10). As mentioned by previous studies[1,24,43], during the 2000–2014/2016 period, the SAM trend was positive, the IPO was in its negative phase and the Atlantic multidecadal oscillation (AMO) was in its positive phase (Supplementary Fig. S10a). All these large-scale climate variabilities correspond to enhanced westerlies and negative wind stress curl anomalies over the SO (Supplementary Fig. S10b). On decadal timescales, these anomalous wind stress and wind stress curls enhance SO upwelling that can bring subsurface warm water to the surface[43]. The subpolar gyre also spins up due to negative wind stress curl anomalies, which can advect warm water from relatively low latitude to the high latitude. The wind-driven vertical and horizontal temperature advections mutually contribute to the heat buildup in the subsurface ocean (Supplementary Fig. S10c).

Given the preconditioning of persistent sea ice declines by the subsurface heat buildup and surface salinification, we speculate that the ocean stratification (density difference between 400 and 0 m) before 2016ND may control the magnitude of this sea ice shift. We therefore show in Fig. 2g, h the scatter plot of ocean stratification averaged from 2014 to 2016 versus the SIE difference between the negative states (2017–2020) and the positive states (2012–2015) based on 30 ensemble members in SPEAR_atm_sst_restore. We can see the ensemble members with larger sea ice differences correspond to weaker ocean stratification anomalies during 2014–2016 in both the SO and Weddell Sea (Fig. 2g, h). Physically, the larger surface salt or subsurface heat perturbations and therefore weaker ocean stratification are more likely to destabilize the upper ocean and cause large sea ice anomalies and vice versa.

To further confirm the important role of ocean conditions in the Antarctic SIE shift, we conduct a sensitivity experiment (SPEAR_atm_restore_2015_newIC) based on our SPEAR_atm_restore, in which the ocean condition in Jan 1 2015 is replaced by another year (we choose year 2007 when the subsurface water is cool, see "Methods"). In the original SPEAR_atm_restore, the SIE decline persists for several years after 2016 in both the SO and Weddell Sea. The averaged SIE anomalies over the 2017–2020 period are negative (Fig. 3a, b). In contrast, the positive SIE anomalies frequently occur after 2016 when the subsurface ocean condition was changed to cold states in 2015. The averaged SIE anomalies over the 2017–2020 period become weakly positive. These sharp differences suggest that the subsurface warming before 2016 plays a crucial role in the sustained SIE low after 2016. Interestingly, the record low SIE in 2016ND is reproduced very well even when we initialize with the cold conditions, which accounts for ~90% of the
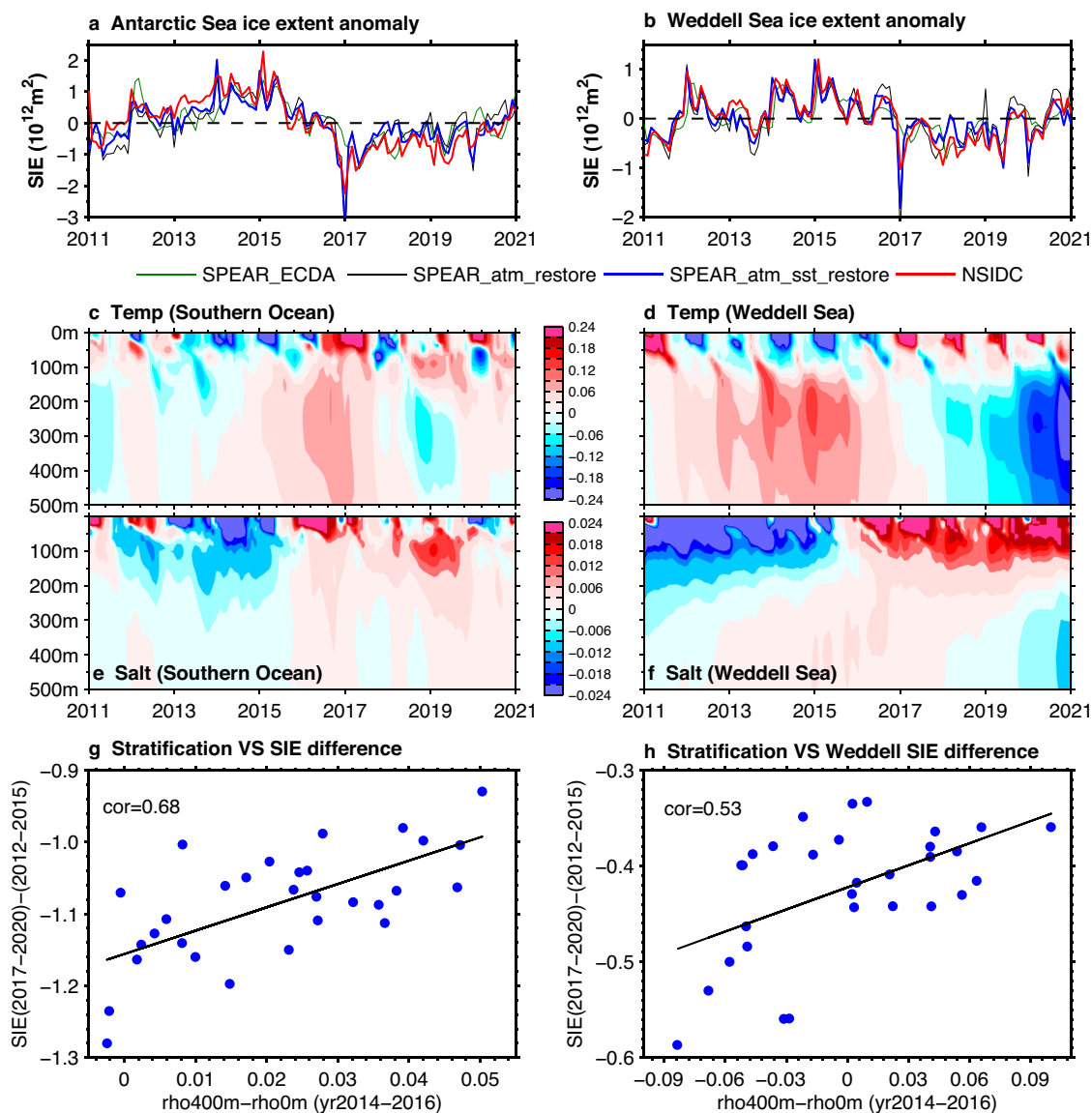
Fig. 2 Ocean changes associated with the Antarctic Sea ice extent (SIE) shift. a Monthly mean SIE anomaly in National Snow and Ice Data Center (NSIDC) observation (red line), SPEAR_ECDA (green line), SPEAR_atm_restore (black line), and SPEAR_atm_sst_restore (blue line). **c** Time-depth evolutions of the monthly Southern Ocean (SO) area averaged (60°S-70°S, 0°E-360°E) temperature anomalies in SPEAR_atm_sst_restore. **e** Same as (**c**) but for the salinity anomalies. **g** Scatter plot of the SO ocean stratification (defined as the density difference between 400 m and 0 m) averaged in time period 2014-2016 versus the Antarctic SIE difference (between 2017-2020 and 2012-2015). (**b**), (**d**), (**f**), and (**h**) are the same as (**a**), (**c**), (**e**), and (**g**) but for the Weddell Sea (55°S-74°S, 50°W-10°E). All anomalies are with respect to the 2011-2020 climatology. Units for the SIE, ocean temperature, salinity, and density are $10^{12}m^2$, °C, PSU, and kgm^{-3}, respectively.

low SIE in SPEAR_atm_restore. This enhances our argument in the last section that the subsurface SO prior to 2016 contributes very little to the sea ice extreme event in late 2016, and that this event was essentially driven by the atmospheric forcing.

Figure 2g, h and the sensitivity experiment (SPEAR_atm_restore_2015_newIC) also indicate a potential predictability of the recent SIE shift since they relate the current ocean state to the future sea ice evolutions. This motivates us to investigate our decadal hindcasts/forecasts that are initialized from SPEAR_atm_sst_restore on January 1 every year (see "Methods" for more model details). Figure 4a, b displays the decadal prediction initialized in 2014, 2015, and 2016 for the total Antarctic SIE and Weddell SIE, respectively, along with the ice time series in observation and SPEAR_atm_sst_restore. All hindcasts produce small SIE values after 2016. The hindcasts initialized in 2014 and 2015 capture a large part of the recent SIE shift, moving the high

sea ice states to average level. We also see that none of the hindcasts produced the record-breaking SIE decline in late 2016 (Fig. 4a). The hindcast initialized on 1 January 2016 only produces a very small SIE low in late 2016, which accounts for ~10% of the record low SIE. The hindcasts initialized in 2015 and 2014 have even less skill in predicting the 2016 extreme event. These phenomena suggest that the initial ocean condition plays a small role in the ND2016 sea ice extreme event, consistent with our arguments above and previous studies[50]. This is not surprising, since the internal atmosphere variability such as the SAM is hard to predict on multiyear timescales. On the other hand, the successful prediction of part of the observed sea ice difference (2017–2020 minus 2012–2015) largely arises from the correct initialization of subsurface heat reservoir (Fig. 4c, d). The initialization captures the subsurface heat evolutions very well primarily due to the long memory of subsurface ocean. The
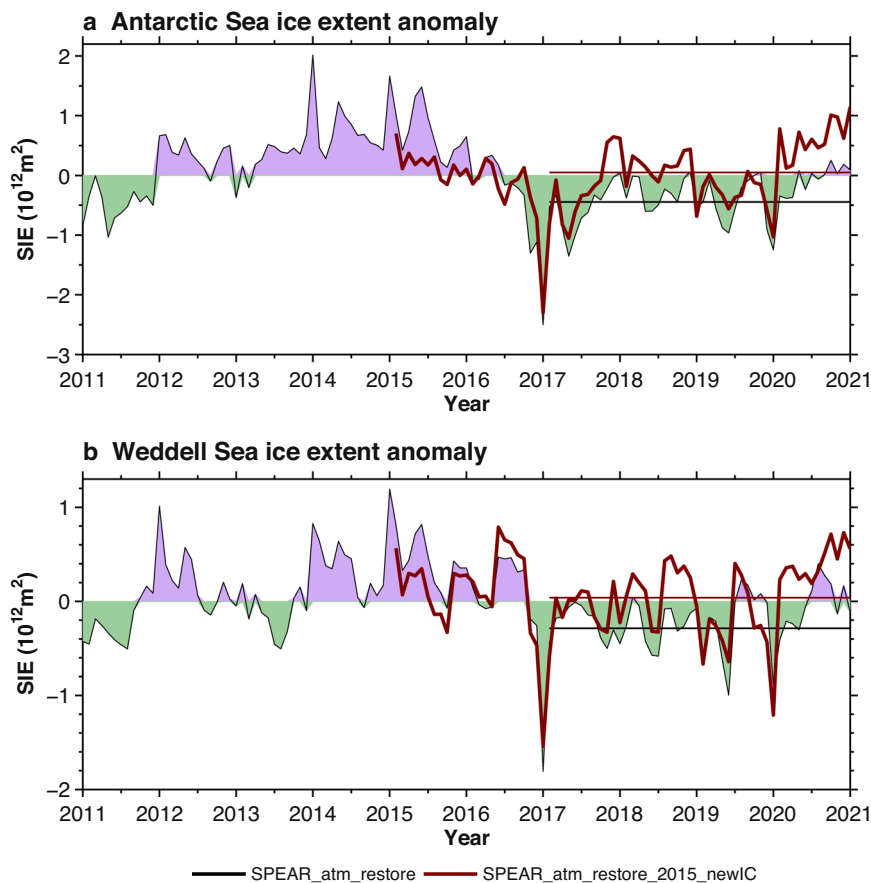
Fig. 3 Role of ocean initial condition in the Sea ice extent (SIE). a The total Antarctic SIE anomaly for the time period 2011–2020 (shading) and the time-averaged (2017–2020) SIE anomalies (horizontal black line) in SPEAR_atm_restore. The brown lines denote the SIE time series and time-averaged (2017–2020) SIE anomalies in SPEAR_atm_restore_2015_newIC. **b** Same as (**a**) but for the Weddell Sea (50°W–10°E). Unit is $10^{12}m^2$. The time-averaged SIE anomalies between two runs (horizontal black and brown lines) in (**a**) and (**b**) are signinficantly different at a 90% confidence level based on the Student's t-test when we concatenate 5 ensemble members.

subsurface heat reduces the ocean stratification, leads to a warm and salty surface water (Supplementary Figs. S11 and 12) and eventually decreases the SIE in the surface ocean. It is worth noting that the subsurface heat can drop the high sea ice states to average level but is not enough to trigger tremendous sea ice declines after 2016. The strong interannual variability of sea ice after 2016 is also missing in the decadal prediction. This means that the subsurface ocean status before 2016 only sustains the overall low states of sea ice after 2016. The tremendous decline of sea ice after 2016 is still largely impacted by the simultaneous atmosphere and ocean variabilities. As mentioned in previous studies[43], the negative SAM trend and positive IPO phase after 2016 can induce surface warming anomalies through southward warm air advection, Ekman warm advection, and Ekman downwelling and in turn decrease the Antarctic SIE. The reoccurrence of Maud Rise Polynya[51,52] observed in 2016 and 2017, which is very likely driven by the strong atmospheric storm events[52] can also enhance the Weddell Sea SIE decline from an ocean perspective. Our SPEAR model underestimates these polynya events probably due to the coarse ocean resolution (~0.5°) in the polar region.

Discussion
In the present study, we have investigated the relative role of subsurface ocean and atmosphere in the recently observed Antarctic SIE declines. It is confirmed that the record low SIE in late 2016 is largely the result of both meridional temperature advection

associated with the zonal wave number 3 teleconnection pattern in the early austral spring induced by tropical SST anomalies and the strong negative SAM event in the late austral spring[38–41], while the subsurface SO plays a much smaller role that only accounts for ~10% of the total change. This argument is supported by three independent model experiments. The first piece of evidence arises from comparing the "perfect" atmosphere simulation with the "perfect" ocean simulation. The former reproduces the record-breaking SIE low very well, while the latter does not. This suggests that the atmosphere and its driven surface ocean and ice variabilities are key for the SIE extreme event. The "perfect" ocean simulation may be questionable due to sparse ocean observations, but our confidence largely enhances as we move to the next two pieces of evidence. The second piece of evidence is from our sensitivity experiment based on SPEAR_atm_restore in which the ocean initial conditions in 2015 were replaced by a cold subsurface state. Even with this change of ocean condition, the record low SIE in late 2016 is reproduced very well that produces ~90% of the SIE low in SPEAR_atm_restore. The third piece of evidence comes from our decadal hindcasts that are initialized from SPEAR_-atm_sst_restore. The hindcast initialized on 1 January 2016 only produces a very small SIE low in late 2016, which accounts for ~10% of the record low SIE in SPEAR_atm_sst_restore. The hindcasts initialized in 2015 and 2014 have even less skill in predicting the 2016 extreme event. The second and third evidence further confirm that the record low SIE in late 2016 is not dependent on prior ocean conditions.
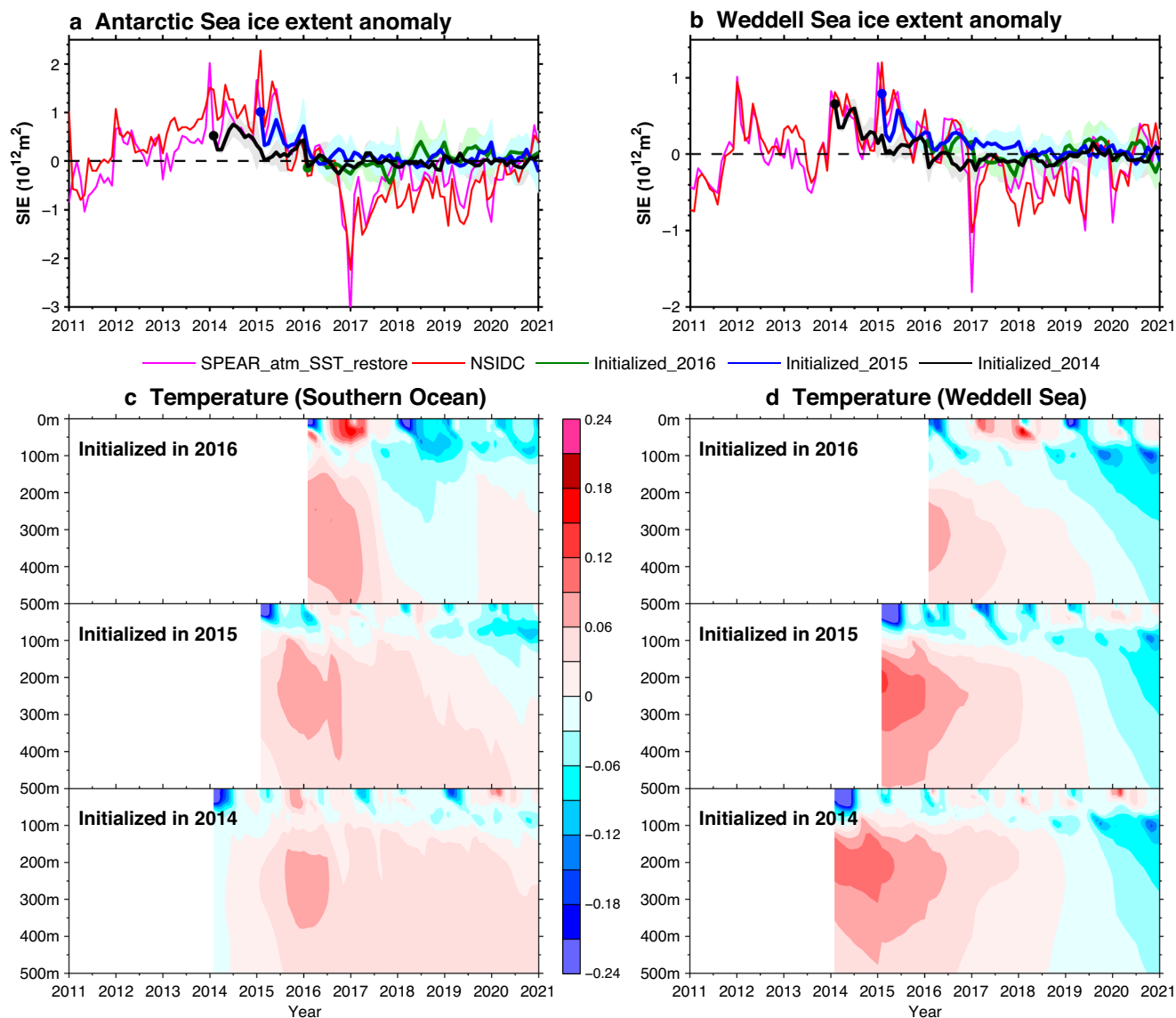
Fig. 4 Decadal hindcasts of Sea ice extent (SIE) and subsurface ocean temperature. a Decadal hindcasts of the total Antarctic SIE initialized in 2014 (black), 2015 (blue), and 2016 (green) along with the SIE time series in SPEAR_atm_sst_restore (magenta line) and National Snow and Ice Data Center (NSIDC) (red line). Lines in the decadal hindcast denote the ensemble mean result, while the shadings denote the ensemble spread represented by the one standard deviation. **c** Decadal hindcasts of ensemble mean Southern Ocean (60°S–70°S, 0°E–360°E) area averaged subsurface temperature evolutions initialized in 2016, 2015, and 2014. **b** and **d** are the same as (**a**) and (**c**) but for the Weddell Sea (55°S–74°S, 50°W–10°E). Units for the SIE and ocean temperature are $10^{12} m^2$, °C, respectively.

In contrast, the subsurface ocean plays a crucial role in the continued Antarctic SIE lows over the last decade. The persistent SIE lows after 2016 are preceded by subsurface warming. This warming is largely due to an enhanced westerly wind trend and thus negative wind stress curl anomalies over the SO in 2000–2015 that leads to an enhanced upwelling and a spin up of subpolar gyres. Our decadal hindcasts initialized in 2014 and 2015 indicate that approximately half of the SIE difference (low ice states in 2017–2020 and high ice states in 2012–2015) can be attributable to this subsurface warming. The subsurface warming persists, gradually destabilizes the ocean from below and in turn moves the high SIE states to the average level. Our sensitivity experiment also points out that the sea ice difference would disappear if the subsurface ocean before 2016 was replaced by cold conditions. This subsurface heat therefore provides a potential prediction source for the recent SIE shift due to the long memory of subsurface ocean. However, we note the subsurface

heat only accounts for approximately half of the SIE difference. The other half still arises from the simultaneous atmosphere, ocean, and/or their coupled variabilities. After 2016, the negative SAM trend, the positive phase of IPO, the occurrence of Maud Rise polynyas and potentially other factors can further amplify the SIE decline. Prediction of these simultaneous climate features requires shorter timescale prediction systems and were likely unpredictable on multiyear timescales. Thus, a combined decadal[46], seasonal[53], and even sub-seasonal[54] prediction system may be needed to better characterize the further evolutions of Antarctic SIE. Observations and our SPEAR simulations also show that the persistent sea ice declines over the recent years mainly occur over the Weddell Sea. This suggests that the Weddell Sea is very critical to control the total Antarctic SIE evolutions in the future. However, the Argo observations over this ice-covered region are very sparse compared to other areas (Supplementary Fig. S7). This calls for improved and sustained

measurements of the subsurface Weddell Sea using new technologies, which could yield substantial benefits in terms of understanding and predicting future Antarctic SIE evolutions.

Methods

Observations. Here we use the National Snow and Ice Data Center (NSIDC) dataset[55] to calculate the SIC spatial pattern, SIE time series and trend. SIE is defined as the cumulative area of all grid cells having at least 15% SIC. The observed subsurface temperature and salinity profiles are calculated from the Met Office Hadley Centre's EN4[49] version 2.4 reanalysis.

Model. We use one model from a new set of coupled ocean-atmosphere models developed at the Geophysical Fluid Dynamics Laboratory (GFDL) (Table 1). The set is collectively called SPEAR (Seamless system for Prediction and Earth System Research)[45]. In this study, we use the low ocean resolution version from this set of models, called SPEAR_LO. The ocean and sea ice components are based on the MOM6 code[56] and have a horizontal resolution of ~1° in the subtropics, with refinements to 0.5° at high latitudes and with meridional refinements to 1/3° in the tropics. The ocean model has 75 layers with layer thickness as fine as 2 m near the surface. The physical configurations in the atmospheric and land components are identical to the newly developed GFDL AM4-LM4 model[57,58], except that we use the retuned near-infrared isotropic reflectance parameter for cold snow over glacial surfaces.

The SPEAR_LO model is then partially constrained by atmospheric observations and/or ocean observations targeting for initializing decadal or seasonal prediction system[46]. We have three different reanalysis datasets based on this SPEAR_LO model. The first dataset is SPEAR_atm_sst_restore, in which the 6-h atmospheric winds and temperature were restored toward atmospheric data from the 55-year Japanese Reanalysis (JRA-55)[59] and the SST within 60°S–60°N was restored toward the time-varying observations from NOAA Extended Reconstructed Sea Surface Temperature version 5 (ERSSTv5) data[60]. The strength of the restoring is tapered linearly from 1.0 at 55°N(S) to 0.0 at 60°N(S) and is equivalent to a 10-day restoring timescale for a 50-m mixed layer depth, corresponding to an effective restoring rate of about 240 W/(m²K). This reanalysis has 30 ensemble members. The second dataset is SPEAR_atm_restore, which is identical to the SPEAR_atm_sst_restore but without SST restoring. We find that the SST restoring does not have too many effects on the Antarctic SIE time series for the timescales assessed here. Thus, we deem these two restoring analyses as the "perfect" atmosphere forcing runs. The third reanalysis we used here is called SPEAR_ECDA, which includes the ocean data assimilation (ODA) system in MOM6 as its backbone, incorporates the ocean tendency adjustment (OTA) bias correction scheme and has a free atmosphere[61]. MOM6 ODA uses the two-step Ensemble Adjustment Kalman Filter (EAKF) that is an ensemble-based sequential assimilation scheme that facilitates parallel implementation of online filter computation. We consider this SPEAR_ECDA as the "perfect" ocean reanalysis. Note that the sea ice component in these three reanalyses is not constrained by observations and primarily responds to atmospheric and ocean variations.

We conduct a sensitivity experiment to examine the role of ocean initial condition in the Antarctic SIE shift in recent years. This run is identical to the SPEAR_atm_restore reanalysis except that the ocean conditions on 1 January 2015 is replaced by that in another year. Here we choose the ocean conditions on 1 January 2007 when the subsurface ocean is relatively cool, which is in stark contrast to the warm subsurface ocean in 2015. This new run is named as SPEAR_atm_restore_2015_newIC.

We also conducted a decadal retrospective forecast using the SPEAR_LO model initialized from SPEAR_atm_sst_restore[46]. A 20-member ensemble of retrospective forecasts was initialized on 1 January every year from 1961 to 2021 and integrated for 10 years with the temporally varying anthropogenic and natural forcing as in the historical simulation. To effectively remove the climate drift assuming that the climate drift is systematic as a function of forecast lead time, the forecast anomalies for each variable were obtained by subtracting out the lead-time-dependent climatology from forecasts.

Data availability

The NSIDC NASA Team Sea ice concentration and area data are available at http://nsidc.org/data/NSIDC-0051. The Hadley Centre's EN4 data set is available at http://www.metoffice.gov.uk/hadobs/en4. The Japanese 55-year Reanalysis JRA-55 is available at https://jra.kishou.go.jp/JRA-55/index_en.html. The ERSSTv5 is available at https://www.ncei.noaa.gov/products/extended-reconstructed-sst. The data for figures are available online at https://doi.org/10.5281/zenodo.7278208.

Code availability

The source code of ocean component MOM6 of SPEAR_LO model is available at https://github.com/NOAA-GFDL/MOM6.

References

1. Eayrs, C., Li, X., Raphael, M. N. & Holland, D. M. Rapid decline in Antarctic sea ice in recent years hints at future change. *Nat. Geosci.* **14**, 460–464 (2021).
2. Parkinson, C. & Cavalieri, D. Antarctic sea ice variability and trends. *Cryosphere Discuss.* **6**, 931–956 (2012).
3. Cavalieri, D. J. & Parkinson, C. L. Antarctic sea ice variability and trends, 1979–2006. *J. Geophys. Res. Oceans* **113**, C07004 (2008).
4. Goosse, H., Lefebvre, W., de Montety, A., Crespin, E. & Orsi, A. H. Consistent past half-century trends in the atmosphere, the sea ice and the ocean at high southern latitudes. *Clim. Dynam.* **33**, 999–1016 (2009).
5. Hobbset, W. R. et al. A review of recent changes in Southern Ocean sea ice, their drivers and forcings. *Glob. Planet. Change* **143**, 228–250 (2016).
6. Jones, J. M. et al. Assessing recent trends in high-latitude Southern Hemisphere surface climate. *Nat. Clim. Change* **6**, 917–926 (2016).
7. Comiso, J. C. et al. Positive trend in the Antarctic sea ice cover and associated changes in surface temperature. *J. Clim.* **30**, 2251–2267 (2017).
8. Liu, J., Curry, J. A. & Martinson, D. G. Interpretation of recent Antarctic Sea ice variability. *Geophys. Res. Lett.* **31**, 2000–2003 (2004).
9. Stammerjohn, S., Martinson, D. G., Smith, R., Yuan, X. & Rind, D. Trends in Antarctic annual sea ice retreat and advance and their relation to El Niño-Southern Oscillation and Southern Annular Mode variability. *J. Geophys. Res.* **113**, C03S90 (2008).
10. Simpkins, G. R., Ciasto, L. M. & England, M. H. Observed variations in multidecadal Antarctic Sea ice trends during 1979–2012. *Geophys. Res. Lett.* **40**, 3643–3648 (2013).
11. Matear, R. J., O'Kane, T. J., Risbey, J. S. & Chamberlain, M. Sources of heterogeneous variability and trends in Antarctic sea-ice. *Nat. Commun.* **6**, 8656 (2015).
12. Maksym, T. Arctic and Antarctic Sea ice change: contrasts, commonalities, and causes. *Annu. Rev. Mar. Sci.* **11**, 187–213 (2019).
13. Stroeve, J., Holland, M. M., Meir, W., Scambos, T. & Serreze, M. Arctic sea ice decline: faster than forecast. *Geophys. Res. Lett.* **34**, L09501 (2007).
14. Meehl, G. A., Arblaster, J. M., Bitz, C. M., Chung, C. T. Y. & Teng, H. Antarctic sea-ice expansion between 2000 and 2014 driven by tropical Pacific decadal climate variability. *Nat. Geosci.* **9**, 590–595 (2016).
15. Turner, J. et al. Non-annular atmospheric circulation change induced by stratospheric ozone depletion and its role in the recent increase of Antarctic sea ice extent. *Geophys. Res. Lett.* **36**, L08502 (2009).
16. Sigmond, M. & Fyfe, J. C. Has the ozone hole contributed to increased Antarctic sea ice extent. *Geophys. Res. Lett.* **37**, L18502 (2010).
17. Purich, A., Cai, W., England, M. H. & Cowan, T. Evidence for link between modelled trends in Antarctic sea ice and underestimated westerly wind changes. *Nat. Commun.* **7**, 10409 (2016).
18. Purich, A. et al. Tropical Pacific SST drivers of recent Antarctic sea ice trends. *J. Clim.* **29**, 8931–8948 (2016).
19. Li, X., Holland, D. M., Gerber, E. P. & Yoo, C. Impacts of the north and tropical Atlantic Ocean on the Antarctic Peninsula and sea ice. *Nature* **505**, 538–542 (2014).
20. Lee, S.-K. et al. Wind-driven ocean dynamics impact on the contrasting sea-ice trends around West Antarctica. *J. Geophys. Res. Oceans* **122**, 4413–4430 (2017).
21. Holland, P. R. & Kwok, R. Wind-driven trends in Antarctic sea-ice drift. *Nat. Geosci.* **5**, 872–875 (2012).
22. Li, X. et al. Tropical teleconnection impacts on Antarctic climate changes. *Nat. Rev. Earth Environ.* **2**, 680–698 (2021).
23. Haumann, F. A., Gruber, N., Münnich, M., Frenger, I. & Kern, S. Sea-ice transport driving Southern Ocean salinity and its recent trends. *Nature* **537**, 89–92 (2016).
24. Purich, A. et al. Impacts of broad-scale surface freshening of the Southern Ocean in a coupled climate model. *J. Clim.* **31**, 2613–2632 (2018).
25. de Lavergne, C., Palter, J. B., Galbraith, E. D., Bernardello, R. & Marinova, I. Cessation of deep convection in the open Southern Ocean under anthropogenic climate change. *Nat. Clim. Change* **4**, 278–282 (2014).
26. Swart, N. C. & Fyfe, J. C. The influence of recent Antarctic ice sheet retreat on simulated sea ice area trends. *Geophys. Res. Lett.* **40**, 4328–4332 (2013).
27. Bintanja, R., Van Oldenborgh, G. J., Drijfhout, S. S., Wouters, B. & Katsman, C. A. Important role for ocean warming and increased iceshelf melt in Antarctic sea-ice expansion. *Nat. Geosci.* **6**, 376–379 (2013).
28. Bronselaer, B. et al. Change in future climate due to Antarctic meltwater. *Nature* **564**, 53–58 (2018).

29. Polvani, L. M. & Smith, K. L. Can natural variability explain observed Antarctic sea ice trends? New modeling evidence from CMIP5. *Geophys. Res. Lett.* **40**, 3195–3199 (2013).

30. Singh, H., Polvani, L. & Rasch, P. Antarctic sea ice expansion, driven by internal variability, in the presence of increasing atmospheric CO_2. *Geophys. Res. Lett.* **46**, https://doi.org/10.1029/2019GL083758 (2019).

31. Zhang, L., Delworth, T. L., Cooke, W. & Yang, X. Natural variability of Southern Ocean convection as a driver of observed climate trends. *Nat. Clim. Change* **9**, 59–65 (2019).

32. Bilgen, S. I. & Kirtman, B. P. Impact of ocean model resolution on understanding the delayed warming of the Southern Ocean. *Environ. Res. Lett.* **15**, 114012 (2020).

33. Sun, S. & Ian, E. Observed Antarctic sea ice expansion reproduced in a climate model after correcting biases in sea ice drift velocity. *Nat. Commun.* **12**, 1–6 (2021).

34. Blanchard-Wrigglesworth, E., Roach, L. A., Donohoe, A. & Ding, Q. Impact of winds and Southern Ocean SSTs on Antarctic sea ice trends and variability. *J. Clim.* **34**, 949–965 (2021).

35. Fogt, R. L., Sleinkofer, A. M., Raphael, M. N. & Handcock, M. S. A regime shift in seasonal total Antarctic sea ice extent in the twentieth century. *Nat. Clim. Change* **12**, 54–62 (2022).

36. Handcock, M. S. & Raphael, M. N. Modeling the annual cycle of daily Antarctic sea ice extent. *Cryosphere Discuss.* **14**, 2159–2172 (2019).

37. Parkinson, C. L. A 40-y record reveals gradual Antarctic sea ice increases followed by decreases at rates far exceeding the rates seen in the Arctic. *Proc. Natl Acad. Sci. USA* **116**, 14414–14423 (2019).

38. Stuecker, M. F., Bitz, C. M. & Armour, K. C. Conditions leading to the unprecedented low Antarctic sea ice extent during the 2016 austral spring season. *Geophys. Res. Lett.* **44**, 9008–9019 (2017).

39. Schlosser, E., Haumann, F. A. & Raphael, M. N. Atmospheric influences on the anomalous 2016 Antarctic sea ice decay. *Cryosphere* **12**, 1103–1119 (2018).

40. Turner, J. et al. Unprecedented springtime retreat of Antarctic sea ice in 2016. *Geophys. Res. Lett.* **44**, 6868–6875 (2017).

41. Wang, G. et al. Compounding tropical and stratospheric forcing of the record low Antarctic sea-ice in 2016. *Nat. Commun.* **10**, 13 (2019).

42. Purich, A. & England, M. H. Tropical teleconnections to Antarctic sea ice during austral spring 2016 in coupled pace-maker experiments. *Geophys. Res. Lett.* **46**, 6848–6858 (2019).

43. Meehl, G. A. et al. Sustained ocean changes contributed to sudden Antarctic sea ice retreat in late 2016. *Nat. Commun.* **10**, 14 (2019).

44. Turner, J. et al. Record low Antarctic sea ice cover in February 2022. *Geophys. Res. Lett.* **49**, e2022GL098904 (2022).

45. Delworth, T. L. et al. SPEAR-the next generation GFDL modeling system for seasonal to multidecadal prediction and projection. *J. Adv. Model. Earth Syst.* **12**, e2019MS001895 (2020).

46. Yang, X. et al. On the development of GFDL's decadal prediction system: initialization approaches and retrospective forecast assessment. *J. Adv. Model. Earth Syst.* **13**, https://doi.org/10.1029/2021MS002529 (2021).

47. Zhang, L. et al. The dependence of internal multidecadal variability in the Southern Ocean on the ocean background mean state. *J. Clim.* **34**, https://doi.org/10.1175/JCLI-D-20-0049.1 (2021).

48. Dufour, C. O. et al. Preconditioning of the Weddell Sea polynya by the ocean mesoscale and dense water overflows. *J. Clim.* **30**, 7719–7737 (2017).

49. Good, S. A., Martin, M. J. & Rayner, N. A. EN4: quality controlled ocean temperature and salinity profiles and monthly objective analyses with uncertainty estimates. *J. Geophys. Res.: Oceans* **118**, 6704–6716 (2013).

50. Kusahara, K., Reid, P., Williams, G. D., Massom, R. & Hasumi, H. An ocean-sea ice model study of the unprecedented Antarctic Sea ice minimum in 2016. *Environ. Res. Lett.* **13**, 084020 (2018).

51. Turner, J. et al. Recent decrease of summer sea ice in the Weddell Sea, Antarctica. *Geophys. Res. Lett.* **47**, e2020GL087127 (2020).

52. Campbell, E. C. et al. Antarctic offshore polynyas linked to Southern Hemisphere climate anomalies. *Nature* **570**, 319–325 (2019).

53. Bushuk, M. et al. Seasonal prediction and predictability of regional Antarctic sea ice. *J. Clim.* **34**, 6207–6233 (2021).

54. Xiang, B. et al. S2S prediction in GFDL SPEAR: MJO diversity and teleconnections. *Bull. Am. Meteor. Soc.* https://doi.org/10.1175/BAMS-D-21-0124.1 (2021).

55. Cavalieri, D. J., Parkinson, C. L., Gloersen, P. & Zwally, H. J. Sea Ice Concentrations from Nimbus-7 SMMR and DMSP SSM/I-SSMIS Passive Microwave Data, Version 1. Boulder, Colorado USA. NASA National Snow and Ice Data Center Distributed Active Archive Center. https://doi.org/10.5067/8GQ8LZQVL0VL (1996).

56. Adcroft, A. et al. The GFDL global ocean and sea ice model OM4.0: Model description and simulation features. *J. Adv. Model. Earth Syst.* **11**, 3167–3211 (2019).

57. Zhao, M. et al. The GFDL Global atmosphere and land model AM4.0/LM4.0: 1. Simulation characteristics with prescribed SSTs. *J. Adv. Model. Earth Syst.* **10**, 691–734 (2018).

58. Zhao, M. et al. The GFDL Global atmosphere and land model AM4.0/LM4.0: 2. Model description, sensitivity studies, and tuning strategies. *J. Adv. Model. Earth Syst.* **10**, 735–769 (2018).

59. Kobayashi, S. et al. The JRA-55 reanalysis: general specifications and basic characteristics. *J. Meteor. Soc. Japan* **93**, 5–48 (2015).

60. Huang, B. et al. Extended Reconstructed Sea Surface Temperature, Version 5 (ERSSTv5): upgrades, validations, and intercomparisons. *J. Clim.* **30**, 8179–8205 (2017).

61. Lu, F. et al. GFDL's SPEAR seasonal prediction system: initialization and ocean tendency adjustment (OTA) for coupled model predictions. *J. Adv. Model. Earth Syst.* **12** https://doi.org/10.1029/2020MS002149 (2020).

Author contributions
L.Z. conceived the initial idea, performed the analysis and sensitivity experiments, and wrote the first draft. T.L.D., X.Y., F.Z., and L.Z. lead the development of SPEAR decadal prediction system. F.L. lead the development of SPEAR_ECDA reanalysis. T.L.D., X.Y., Y.M., and M.B. provided extremely valuable suggestions and comments for the paper. All authors contributed to the improvement of the manuscript.

Competing interests
The authors declare no competing interests.

Additional information
Supplementary information The online version contains supplementary material available at https://doi.org/10.1038/s43247-022-00624-1.

Correspondence and requests for materials should be addressed to Liping Zhang.

Peer review information *Communications Earth & Environment* thanks Gerald Meehl and the other, anonymous, reviewer(s) for their contribution to the peer review of this work. Primary Handling Editors: Aliénor Lavergne.

Reprints and permission information is available at http://www.nature.com/reprints

Publisher's note Springer Nature remains neutral with regard to jurisdictional claims in published maps and institutional affiliations.